Coefficient-of-Performance Analyses for Light-Emitting-Diode Cycles Resembling Carnot Heat Pumps

JIHONG ZHANG[1] AND TIENMO SHIH[2,3]

[1]School of Electromechanical and Automotive Engineering, Yantai University, Yantai 264005, China
[2]Department of Physics, Xiamen University, Xiamen 361005, China
[3]Tianming Physics Research Institute, Changtai 363900, Fujian, China

Corresponding author: Tienmo Shih (tshih111@gmail.com)

ABSTRACT Designing the light-emitting diodes (LEDs) that yield maximal coefficients of performance (ξ_{max}) subject to prescribed electrical powers constitutes a desirable and challenging task. In this paper, via an analogy between the reverse Carnot cycle and the LED cycle, we have identified two distinctive situations. Under normal operations, the electrical power is supplied to allow LED electrons to overcome the p/n junction barrier and is converted to thermal energy rate, which is dissipated to the surroundings. Meanwhile, the LED absorbs the very small amount of thermal energy rate (approximately zero and much smaller than the electrical power) from surroundings as a result of the Peltier effect. Therefore, the maximal light power emitted by the LED must not exceed electrical power (P_{ele}) minus the barrier-overcoming power (IV_{net}). Subsequently, ξ_{max} is obtained as ($P_{ele} - IV_{net})/P_{ele}$. Under relatively unusual situations when LEDs are capable of absorbing sufficient thermal energy rates from surrounding reservoirs (the same order of magnitude as the electrical power), ξ_{max} can possibly exceed the unity, and its expression is theoretically derived in the text. Fundamentally, this paper may contribute to areas of energy saving and light-power illumination.

INDEX TERMS LED cycle, thermal-energy absorption, Carnot heat pumps, temperature gradient, coefficient of performance.

I. INTRODUCTION

In general, for traditional LEDs, only approximately 50% of the electrical power is converted into the emitting light, with the remaining 50% wasted as thermal energy [1], [2]. Clearly, as researchers strive to increase emitting-light percentages, the wasted thermal energy will correspondingly decrease[3]–[5]. Researchers have focused on improving the internal quantum efficiency (IQE) and light extraction efficiency (LEE) of LEDs [6], [7]. Unfortunately, the performance of LEDs continues to suffer from low IQE and LEE. It is gratifying that the availability of LEDs with the efficiency higher than unity has been reported for micro devices[8]–[13]

(e. g. driven by small currents $I \approx O\left(10^{-12}A\right)$). The reason lies in that thermoelectrically pumped LED absorbs thermal energy from the surroundings and converts into light. If the electrical power and the emitted light can be perceived as the work and the energy output (Appendix A) respectively, it is surely possible for these two quantities to equalize, or even for the latter to surpass the former with the condition of absorbing thermal energy from surroundings. This indicates that LED can be perceived as a heat pump when it is driven by small currents [11]. Based on the theory of thermodynamics, the precise definition of the heat pump is determined by the direction of the thermal cycle, but is not dictated by masses of working fluids. For example, in a refrigerator, the flow generally follows the sequence of a compressor, a condenser, an expansion valve, and an evaporator, and the net area
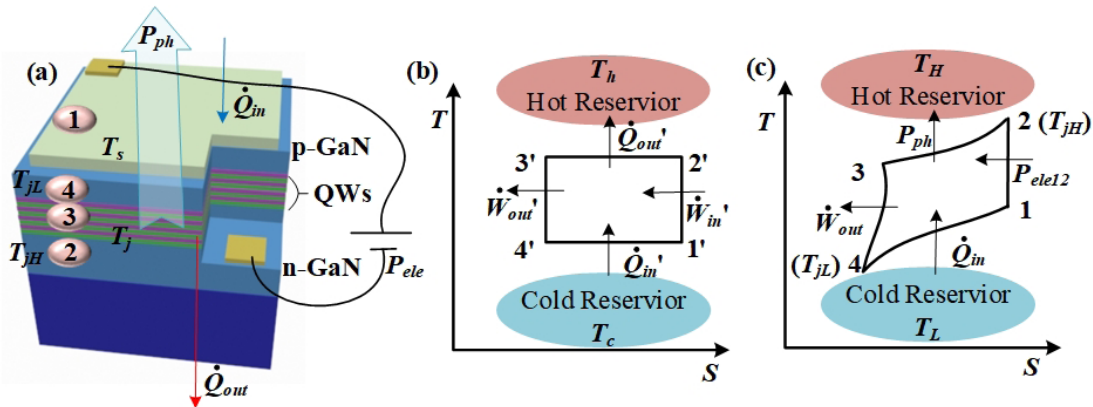
The associate editor coordinating the review of this manuscript and approving it for publication was Kin Kee Chow.

FIGURE 1. Thermal-energy absorption and temperature-gradient existence in an LED cycle. (a) The 3-D representation of an LED cycle that also shows states from 1 to 4. QWs denote quantum wells, and T_S denotes the surface temperature. (b) An analogous reverse Carnot cycle, in which the system absorbs the thermal energy from the cold reservoir and ejects the energy into the hot reservoir. (c) The LED cycle, in which the LED system absorbs the thermal energy from the cold reservoir (adjacent to the surface of LED chip), and emits the light to the surroundings as well as ejects the thermal energy into the hot reservoir (heat sink).

enclosed by the cycle on the Pressure - Volume diagram (or Temperature - Entropy diagram) represents positive net heat transfer. Therefore, LED cycle can be perceived as a reversed thermal cycle (or a heat pump) regardless of the number of transporting electrons (or the amount of driving currents).

II. ANALOGY AND PHENOMENA

Under normal operational conditions of LED, since the light power (P_{ph}) is generally dwarfed by the electrical power (P_{ele}), the remaining portion ($P_{ele} - P_{ph}$) will be converted into the thermal power. Due to the Ohmic heating [14], LED must inevitably generate some thermal energy and discard it to the surroundings when LED is driven by the electrical source. Due to the Peltier's effect [15], by contrast, electrons must overcome P/N-junction barrier and the LED must absorb the energy from the surroundings. The thermal power induced by Ohmic heating equals I^2R, where I denotes the current and R the electrical resistance). The thermal power absorbed by Peltier effect is proportional to the current (I) and the difference between Peltier coefficients of two junction materials. It is usually much smaller than the Ohmic heating and can be neglected in the normal operation of LEDs. However, under small currents [11], [12], it will become significant, and help induce the efficiency of LED to exceed unity. Due to such inevitability of Peltier effect, this energy-absorption process must be legitimately included when LED cycle is analyzed for the sake of rigorousness.

Here we have investigated the energy conversion in LED cycles that contains four processes. In reference to Fig. 1a, LED receives the electricity ($1 \rightarrow 2$), emits the light ($2 \rightarrow 3$), needs to overcome the P/N-junction barrier ($3 \rightarrow 4$), and inevitably absorbs the energy from the surroundings ($4 \rightarrow 1$). Reasonably, electricity, light, barrier overcoming (thus generating excessive thermal energy), and absorbed energy from surroundings can be perceived as work input, light output, heat-transfer output, and heat-transfer input, respectively. Therefore, these four processes constitute a cycle analogously

designed for refrigerators or heat pumps and resemble an idealized reverse Carnot cycle (Fig. 1b).

A refrigeration system undergoes a reverse Carnot cycle [16]–[20], which consists of four processes: (a) $1' \rightarrow 2'$, isentropic compression, (b) $2' \rightarrow 3'$ isothermal compression, (c) $3' \rightarrow 4'$ isentropic expansion, and (d) $4' \rightarrow 1'$, isothermal expansion (Fig. 1b). During this cycle, the entropy of the assembly that comprises the refrigeration system and two reservoirs remains unchanged after a complete cycle is operated. Incidentally, in other words, the cycle is reversible.

Similarly, in the LED cycle, four processes including work input (electrical power), light output (optical power), heat-transfer output (thermal power), and heat-transfer input (Peltier effect) are included. All these four processes, namely the carrier injection process (work input), the recombination process (light output), the P/N-junction barrier overcoming process (Ohmic heating induced heat-transfer output and Peltier effect induced thermal input), occur at the junction active region. To further understand the LED cycle, we have sequentially analyzed these four process individually via the analogy to the Carnot cycle.

Electrons travel through a battery (or other electrical sources) ($1 \rightarrow 2$) and a portion of the work is injected into the system (Fig. 1c and Appendix B) with the abscissa in S and the ordinate in T, resulting in $T_2 > T_1$. This portion of the work is $P_{ele,12}$ that supplies the P/N-junction barrier overcoming in process ($3 \rightarrow 4$). In other words, electrons in LED cannot overcome the P/N-junction barrier unless the LED is driven by a forward voltage. Therefore, $P_{ele,12}$ must exceed the barrier-overcoming power $IV_{net} = I(V_{ext} - V_{bi})$, where V_{ext} denotes the external voltage, and V_{bi} the build-in voltage. Electrons flow from N-type GaN to P-type GaN ($2 \rightarrow 3$) for blue LEDs and the other portion of the work ($P_{ele,23}$) is injected into this LED system (in use for illumination), the light (optical power P_{ph}) is emitted, therefore, the internal-energy variation between state 2 and state 3 obeying $\Delta U_{23} = P_{ele,23} - P_{ph}$. For illustration, in theory let us

consider the case of $\xi = P_{ph}/P_{ele} = 1$ (ξ denotes the coefficient of performance), which implies $P_{ele} = P_{ph}$, we deduce that $\Delta U_{23} = P_{ele,23} - P_{ph} < 0$, indicating that $T_3 < T_2$. Continually, the injected electrons obtained energy from electricity ($1 \rightarrow 2$), then overcome the energy barrier ($3 \rightarrow 4$) while $\dot{W}_{out,34}$ (work out between state 3 and state 4) is delivered to thermally influence the lattice ($\dot{Q}_{out,34}$, thermal power dissipation between state 3 and state 4), which acts as a thermal liaison between the reservoir and electrons. Due to the fact that the internal-energy variation between state 3 and state 4 $\Delta U_{34} = \dot{Q}_{out,34}$, the system temperature must be further lowered, i.e. $T_4 < T_3$. The cold lattice situated on the LED surface absorbs thermal energy from the surroundings ($4 \rightarrow 1$), and afterwards electrons return to the original state ($T_1 > T_4$). Slightly, processes $2 \rightarrow 3$, $3 \rightarrow 4$, and $4 \rightarrow 1$ deviate from those in the reverse Carnot cycle.

We can prove that the entropy change for the assembly is always greater than zero (Appendix C). Since the entropy is regarded as a state property, the entropy change of a system equals zero after the system undergoes a cycle. Hence, for a cycle, we only need to pay our attention to the entropy change of surrounding reservoirs (T_H denotes the temperature of hot reservoir, and T_L the temperature of cold reservoir). According to first and second laws of thermodynamics, we obtain

$$P_{ph} + \dot{Q}_{out} = P_{ele} + \dot{Q}_{in}, \tag{1}$$

and

$$\frac{IV_{net}}{T_H} + \frac{P_{ph}}{T_H} - \frac{\dot{Q}_{in}}{T_L} \geq 0. \tag{2}$$

where $\dot{Q}_{out} = \dot{Q}_{out,34} = \dot{W}_{out,34}$, $V_{net} = V_{ext} - V_{bi}$, $V_{ext} > V_{bi}$ when LED is operated to emit light. Below, it is interesting to determine various maximum COPs when either P_{ele} or $\dot{Q}_{in}$ is a fixed value.

(A) If P_{ele} is a fixed value, we obtain, according to Eq. (1)

$$\xi = \frac{P_{ph}}{P_{ele}} = \frac{P_{ele} + \dot{Q}_{in} - \dot{Q}_{out}}{P_{ele}}.$$

Since $\dot{Q}_{out}$ is no less than IV_{net}, the maximum of ξ is obtained when Q_{in} reaches maximum and $\dot{Q}_{out} = IV_{net}$. In other words, LED can emit the maximum photon power when it can absorb maximum energy from the surroundings.

Based on the inequality (2), we can obtain the maximum $\dot{Q}_{in}$ to be

$$\dot{Q}_{in,max} = (IV_{net} + P_{ph})\frac{T_L}{T_H},$$

which leads to,

$$\xi_{max} = \frac{P_{ele} + (IV_{net} + P_{ph})\frac{T_L}{T_H} - \dot{Q}_{out}}{P_{ele}}. \tag{3}$$

(B) If $\dot{Q}_{in}$ is a fixed value, then

$$\xi = \frac{P_{ele} + \dot{Q}_{in} - \dot{Q}_{out}}{P_{ele}} = 1 + \frac{\dot{Q}_{in} - \dot{Q}_{out}}{P_{ele}}.$$

If $\dot{Q}_{in} \leq \dot{Q}_{out}$, then ξ will become unity as the maximum when P_{ele} approaches infinity, suggesting that

$$\xi_{max} \approx 1. \tag{4}$$

If $\dot{Q}_{in} > \dot{Q}_{out}$, then ξ will become maximum as P_{ele} reaches the minimum. Based on the inequality (2), we obtain the minimum P_{ele} mathematically as

$$P_{ele,min} = \frac{T_H}{T_L}\dot{Q}_{in} - \dot{Q}_{in},$$

which leads to,

$$\xi_{max} = 1 + \frac{1 - \frac{\dot{Q}_{out}}{\dot{Q}_{in}}}{\frac{T_H}{T_L} - 1}. \tag{5}$$

Consequently, in the real life, when a blue LED is driven by 350mA under normal operation, P_{ele} is a fixed value, $\dot{Q}_{in} \approx 0$, $\dot{Q}_{out} \geq IV_{net}$, we obtain, according to Eq. (3),

$$\xi_{max} = \frac{P_{ele} - IV_{net}}{P_{ele}}, \tag{6}$$

since in terms of heat transfer, the absorption rate, $\dot{Q}_{in}$ should equal $Ah\Delta T \approx O\left(10^{-4}W\right) \ll IV_{net} \approx O\left(10^{-1}W\right)$, where A denotes the LED area exposed to the surroundings ($O\left(10^{-6}m^3\right)$) [21]; h the heat-transfer coefficient ($O\left(10W/m^2K\right)$), and ΔT the temperature difference between the LED low junction temperature and the ambient temperature ($\Delta T \approx O\left(10^1K\right)$ is shown in part of experiments and results).

Therefore, if the LED is incapable of absorbing external environmental energy, the maximum P_{ph} can reach only $P_{ele} - IV_{net}$, resulting in a maximal coefficient of performance, satisfying $\xi_{max} = (P_{ele} - IV_{net})/P_{ele}$.

In experiments, we have selected nine high power (1W) LED samples (three blue, three green and three red) to measure COPs that do not exceed 30% when samples are driven in normal conditions. After this selection, we have tested external voltages (V_{ext}) for these LED samples driven by different currents (e.g. 150mA, 250mA, 350mA, 450mA), and tested V_{bi} for these LEDs under small currents (e.g.1μA). We obtained ξ_{max} based on Eq. (6) as shown in Fig. 2b. and as listed in Table 1 for RGB LEDs. In other words, COP of these LED samples cannot exceed these values regardless of the number of quantum wells and the value of external quantum efficiency. To exceed these values, we must design LEDs that can somehow absorb the energy from the surroundings to compensate for the loss of IV_{net}. Under the present LED-manufacturing technology, the smallness of chip areas renders it extremely difficult for LEDs to absorb sufficient energy for normal magnitudes of injected currents ($\sim$100 mA). At very small currents, however, e. g. $I \approx O\left(10^{-12}A\right)$ which leads to $P_{ele} \approx O\left(10^{-12}W\right)$, such an accomplishment can be made possible by reducing IV_{net} to be overwhelmed by absorbed thermal energy ($\approx O\left(10^{-4}W\right)$). Under these circumstances, ξ can even, in principle, exceed unity [11].

It is worth noting that, in principle, under a prescribed electrical power, we can increase the absorbed energy from the
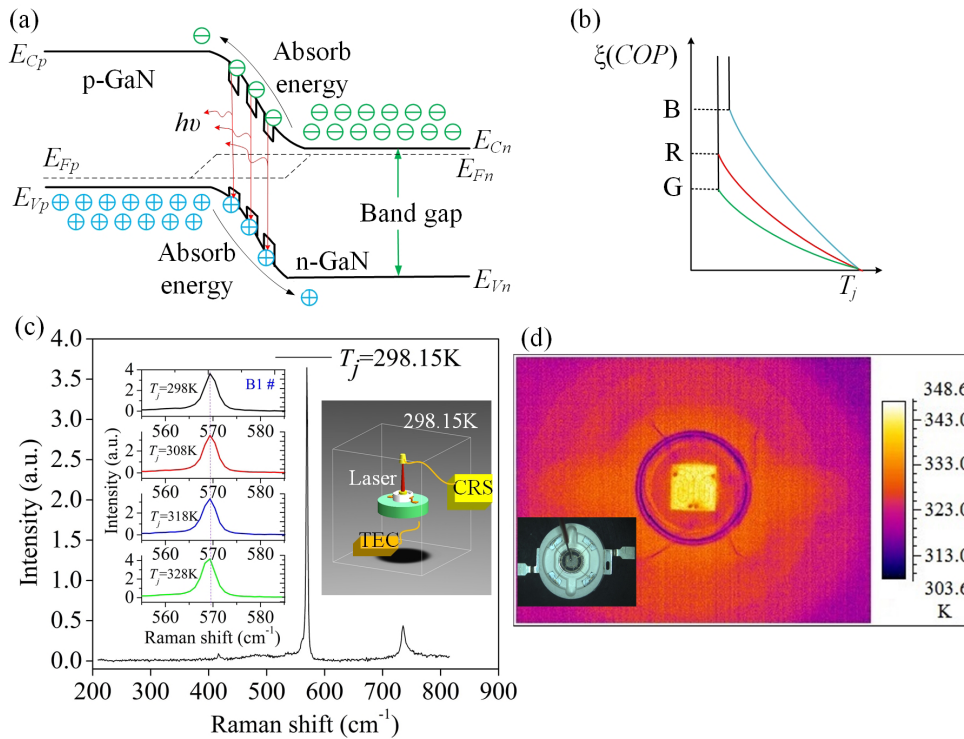
FIGURE 2. Peltier effect and experiments. (a) Band diagram for forward voltages across a P/N-junction. When the photon power approaches the electrical power, carriers must absorb the thermal energy (Q_{in}) from surroundings to overcome the junction barrier. The device operates like a heat pump. (b) COP for RGB LEDs under 350 mA. The built-in electrical field of RGB LEDs are different, resulting in the different values of COPs for Blue, Green and Red LEDs. (c) The relationship (inset on the left) between T_j and the Raman shift for the Blue LED sample when the LED chip is lit under a small current (5 mA). The peak at T_j = 328.15K (this value is simply rounded off as 328K of the inset figure) has shifted to the left slightly when compared with the peak at T_j = 298.15K. Next, at steady state and I = 350 mA, for example, we measure Raman shift to obtain the peak location. Then utilizing the T_j and Raman shift relationship, we obtain T_j = 349.65K (inset on the right showing the experimental set-up of confocal Raman spectroscopy. (d) The infrared image obtained by thermal imager (TI) for a Blue LED sample. The inset shows that the thermocouple (TC) tip is placed on the LED chip to measure surface temperatures. The photo shows the comparison between the size of a TC tip and the LED chip. For the purpose of ensuring sufficient resolutions, the former is chosen to be conspicuously smaller than the latter.

TABLE 1. COPs for RGB LEDs.

current	150mA	250mA	350mA	450mA
ξ for Blue LEDs	80.2%	76.8%	74.0%	71.7%
ξ for Green LEDs	63.1%	60.0%	57.5%	55.4%
ξ for Red LEDs	74.0%	69.9%	66.6%	64.0%

surroundings in order for LEDs to emit as much light as possible, in terms of thermodynamics. However, the absorption rate, $\dot{Q}_{in}$ should equal $Ah\Delta T \approx O\left(10^{-4}W\right)$, where the area A is a fixed value and the heat-transfer coefficient h is about $10\ W/m^2K$ [21], while ΔT is determined by the temperature difference between the LED low junction temperature and the ambient temperature in thermal equilibrium. Hence, it is critical for us to acquire the information of the junction temperature below.

III. JUNCTION TEMPERATURE MEASUREMENTS

In our laboratory, we have adopted the confocal Raman spectroscopy (CRS) [22], thermocouples and a thermal imager to obtain junction temperatures of LEDs (Fig. 2c and d). When using CRS, based on anti-Stokes and Stokes, we measure junction temperature T_j for various currents and materials (Fig. 3a). Nine exposed LEDs (1W each) are selected for experiments, including three blue InGaN/GaN, three green InGaN/GaN and three red AlGaInP. During normal LED operations, the temperature is distributed fairly uniformly (Fig. 3b) with zero gradients within junction semiconductors and nonzero gradients in the internal heat sink (Die attach, cupper slug, grease), which is sandwiched between LED and an external heat sink controlled by a temperature controller (Keithley 2510). Experimental procedures and results are described in Appendix D when the LED is driven in normal operations. When COPs exceed values listed in Table 1, LEDs must absorb the thermal energy from the surroundings. According to Fourier's law for heat conduction, the thermal energy travels from hot to cold bodies spontaneously. The temperature on one side of the LED chip surface (T_{jL}) at state 4 (located at P-type GaN between the chip surface and the depletion zone) must become lower than the ambient temperature, so that the absorption of the thermal energy
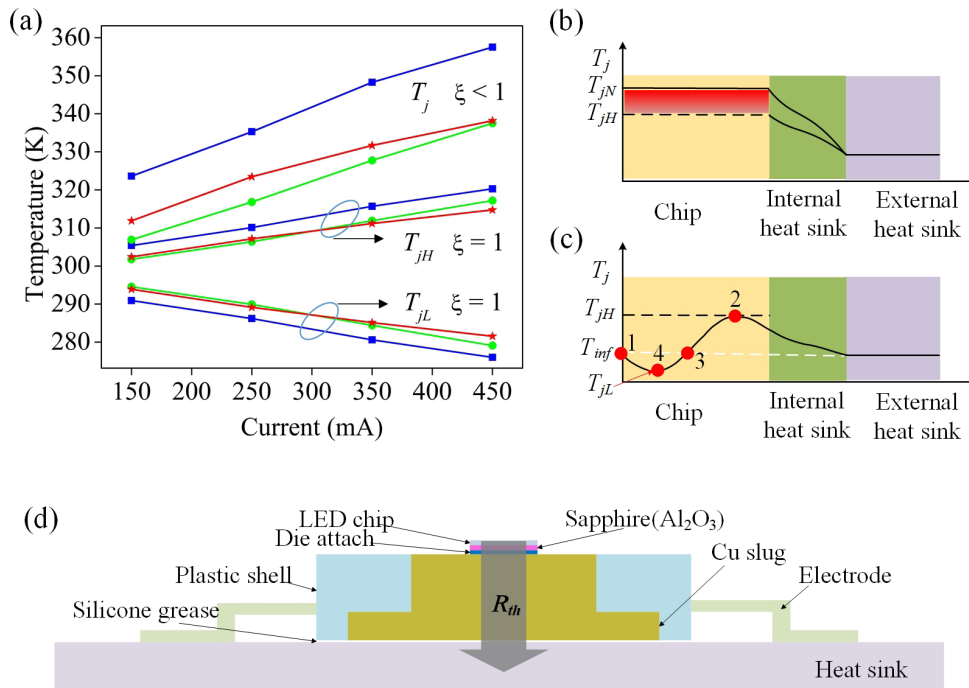
FIGURE 3. Experimental results and junction temperature spatial distributions for LED. (a) Average junction temperatures measured by CRS, TI and TC for various injected-current values at $\xi < 1$. The high junction temperature $T_{jH}(T_{j2})$ and low junction temperature $T_{jL}(T_{j4})$ for $\xi = 1$ are computed based on the thermal-resistance principle and T_j values at $\xi < 1$ (i. e., in the normal operation). (b) Temperature distributions for LED. The LED chip temperature T_{jN} (N denotes "normal operation") appears fairly uniformly with zero gradients under normal operation (COP is approximately 20%). When COP increases gradually from approximately 20% to values in Table 1, T_j will decrease to T_{jH} as thermal power decreases. The chip temperature remains fairly uniform in this decreasing process. (c) Temperature-gradient existence in LED chip. T_{inf} denotes the ambient temperature. LED chip temperatures vary between T_{jH} and T_{jL}. (d) The side-view schematic of the blue LED system.

by LED will occur (Fig. 3c). Reversely, the temperature on the other side of the LED chip (T_{jH}) at state 2 (located at N-type GaN between the depletion zone and the substrate) must become higher than the external heat sink temperature, so that the ejection of the thermal energy by LED will take place. Consequently, the temperature distribution inside the LED chip should qualitatively become non-uniform. We authors are incapable of achieving COP LED (1W) that exceeds the unity (or exceeds other values listed in Table 1) in our laboratory, therefore, we only qualitatively analyze the non-uniform temperature distribution. Quantitatively, we use the thermal-resistance principle to calculate the junction temperature (T_{j2} and T_{j4}) below. These qualitative results show the energy abortion rate, $\dot{Q}_{in}$, is approximately $O\left(10^{-4}W\right) \approx 0$.

For $\xi < 1$ (i. e. in the normal operation), we obtain R_{th} based on the invariant property of thermal resistance in the same LED system [23], namely $R_{th} = \Delta T / P_{th}$ (R_{th} denotes the thermal resistance, ΔT the junction gradient, P_{th} the thermal power), which is used to extrapolate T_j for $\xi = 1$ (Figs. 3a and d).

Based on the first law of thermodynamics we can obtain energy-conservation equations (Appendix E), and based on

the thermal-resistance principle, namely $R_{th} = \Delta T / P_{th} = (T_{j2} - T_{sink})/\dot{Q}_{out}$, we can obtain $T_{j2} = 315.70\text{K}$ (T_{sink} denotes the temperature of heat sink). Therefore, we theoretically obtain $T_{j2} = 315.70\text{K}$, $T_{j4} = 280.60\text{K}$ for $\xi = 1$ of a blue LED driven by $I = 350$ mA.

According to Newton's cooling law for heat convection, $Q_{in} = Ah\Delta T$, for $A \approx 10^{-6}\text{m}^2$ and $h = 10\text{ W/m}^2\text{K}$, we obtain $\Delta T_{max} = T_{sur} - T_{j4} = 298.15\text{K}–280.60\text{K}$. It is nearly impossible for this designed LED to operate at $\xi = 1$ unless the condition is changed, e.g. the absorption rate, $\dot{Q}_{in}$ should equal $Ah\Delta T$ that should reach $O\left(10^{-1}W\right)$. In other words, if all conditions remain unchanged, then ξ can reach only $P_{ph}/P_{ele} = (P_{ele} - IV_{net})/P_{ele} = (1.085–0.282)/1.085 = 74.0\%$ (as shown in Table 1, this number is obtained for blue LED sample, with forward driven current equaling 350mA).

When the driven current remains constant, LED junction temperature should be uniform in the normal operation. However, when ξ reaches unity (or higher than values listed in Table 1), temperature gradients will exist (Figs. 3a, 3c). Consequently, we observe that the deviation between T_{jH} and T_{jL} enlarges as driven currents increase, causing the increase in thermal stresses, which subsequently induce the undesirable aging of LEDs.
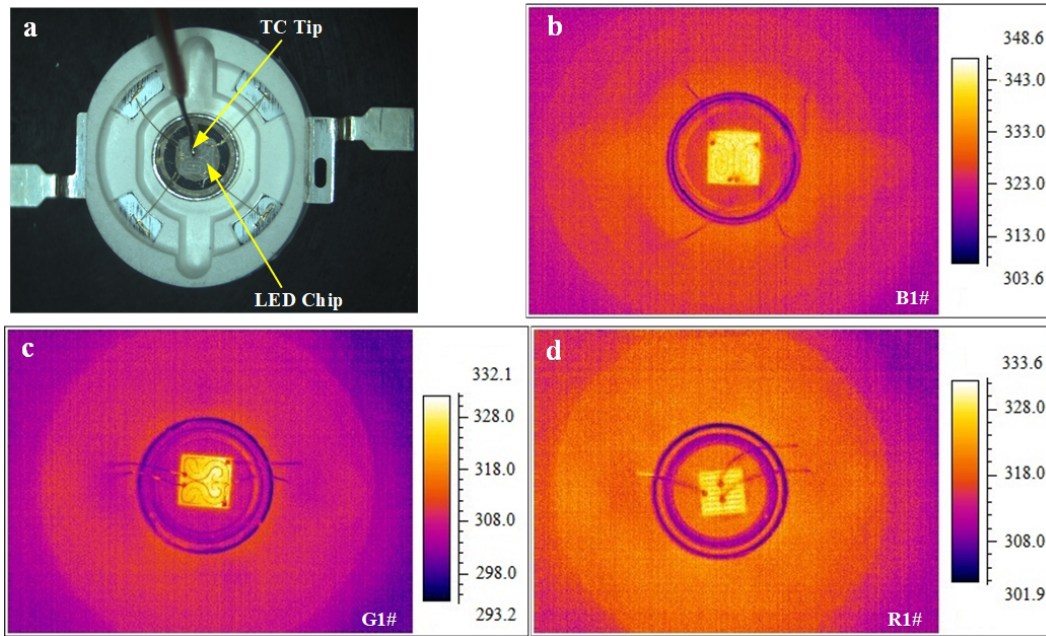
FIGURE 4. Experimental results obtained by thermocouple (TC) and thermal imager (TI). a, The TC tip is placed on the LED chip to measure surface temperatures. The photo shows the comparison between sizes of the TC junction tip and the LED chip. Conspicuously, the former is smaller than the latter, thus ensuring sufficient resolutions. b, The infrared imagery obtained by TI for Blue1# sample. c, The infrared imagery obtained by TI for Green1# sample. d, The infrared imagery obtained by TI for Red1# sample.

IV. CONCLUSION

We have discovered and reported in theories that (1) the maximum coefficient of performance is $\xi_{max} = (P_{ele} - IV_{net})/P_{ele}$ for high power LEDs under normal magnitudes of injected currents ($O\left(10^2 mA\right)$).; (2) the junction-temperature spatial distribution inside LED can range between T_{j2} (T_{jH}) and T_{j4} (T_{jL}) (when $\xi = 1$ in theory for high power LED, $T_{j2} = 315.70K$, $T_{j4} = 280.60K$ for blue LED driven by $I = 350$ mA), while $\dot{Q}_{in}$ that cannot reach $O\left(10^{-1}W\right)$. Therefore it is difficult for COP of LEDs to exceed ξ_{max}; (3) to achieve $P_{ph} = P_{ele}$, we must increase the heat-absorbing capability of LED; and (4) the analogy between the reverse Carnot cycle and LED cycle should facilitate LED-related studies in areas of efficiencies and coefficients of performance.

APPENDIX A

In the LED, the emitted light power should be considered as energy output because (a) it belongs to the thermal radiation, which represents one of three heat transfer modes (conduction, convection, and radiation), (b) In photovoltaic cells, the solar input (energy input) can never exceed the electricity output (work), known as the Shockley-Queisser Limit, (c) Santhanam *et al.* [11] at Massachusetts Institute of Technology, they reported that the light power emitted by LED could possibly exceed the electricity flowing into LED.

APPENDIX B

In the LED, the thermal power is mainly dissipated via heat conduction from the PN junction to the heat sink [24].

When the LED has theoretically reached its COP limit ($\xi_{max} = (P_{ele} - IV_{net})/P_{ele}$) or even higher than the unity, it must dissipate the minimum thermal power (IV_{net}) into the heat sink by the heat conduction. Meanwhile, we notice that the LED must absorb the thermal energy via heat convection and thermal radiation from the surroundings. In other words, the heat transport should be viewed as one way in the LED cycle in fig. 1c.

APPENDIX C

In LED cycle, during $1 \rightarrow 2$, since no heat transfer takes place, the entropy of the assembly remains unchanged.

During $2 \rightarrow 3$, since the temperature of the LED system varies, let us consider instead infinitesimal entropy changes for both the system and the hot reservoir, namely $-\delta P_{ph}/T$ and $\delta P_{ph}/T_H$. Note that the symbol "δ" denotes "depending on the path", and differs from "d". Since T always exceeds T_H, this entropy change is guaranteed to be always greater than zero.

During $3 \rightarrow 4$, according to the Ohmic heating (Fig. 2a), the energy required to overcome the barrier equals IV_{net} ($V_{net} = V_{ext} - V_{bi}$), which inevitably exists during LED operations, and is eventually converted into the wasted thermal energy. Here V_{ext} denotes the voltage externally applied to the system, and V_{bi} denotes the built-in voltage in the P/N-junction. In other words, a portion of electrical power, IV_{net}, is first converted to potential energy of electrons ($\dot{W}_{out}$), then to the lattice's thermal energy ($\dot{Q}_{out}$), which is eventually ejected to the hot reservoir. In other words, $\dot{Q}_{out} = IV_{net}$.

And the entropy change $(-\delta\dot{Q}_{out}/T + \delta\dot{Q}_{out}/T_H)$ is also guaranteed to be always greater than zero.

Without repetition, during the process $4 \rightarrow 1$, we can prove that the entropy change for the assembly is always greater than zero. Since the entropy is regarded as a state property, the entropy change of a system equals zero after the system undergoes a cycle.

APPENDIX D

A. CONFOCAL RAMAN SPECTROSCOPY (CRS)

CRS includes two primary steps: (a) measure Raman shifts for various $T_j = T_{sink}$ (junction temperature = sink temperature) values to obtain a relationship between Raman shift and T_j when LED is lit at small currents (5 mA). The LED sample is mounted on a heat sink, controlled by a temperature controller (Keithley Instruments, Inc., American, Keithley 2510), and is lit by a current source (Keithley Instruments, Inc., American, Keithley 2611). (b) measure Raman shifts to obtain desired T_j when LED is litby large currents. Raman shift signals are collected by a confocal Raman microscope (XploRA, HORIBA Jobin Yvon, France) to yield a correlation between the wave-peak location and the junction temperature when the LED is lit at small currents (5 mA). After the acquisition of this shift and T_j relationship, we turn on the LED at large currents and measure the Stokes shift again. Because the Blue1 chip emits 400 ∼ 550 nm light beams, we select the 633 nm laser, carefully maintain all parametric conditions the same as the small-current run at $T_{sink} = 298.15$K, and measure Raman shifts under currents of 150 mA, 250 mA, and 350 mA.

B. THERMOCOUPLES

Thermocouples (TES-1310 K-type Nickel-chromium alloy and nickel silicon alloy) were used to measure temperatures of exposed LED surfaces (Fig. 4a). The diameter of the thermocouple tip was measured by a vernier caliper to be 0.2 mm, significantly smaller than the area of LED chip (1 mm × 1 mm). Several measurements were taken at random positions on the chip surface to yield the mean value.

C. THERMAL IMAGER

A thermal imager, capable of providing non-intrusive measurements, was used to record the infrared (IR) imagery (25 fps) of the chip surface (Fig. 4b-d), with the distance between the sample and the camera lens being precisely the focal point of camera lens. When the LED sample was unlit, T_{sink} was set to be 343.15 K. At steady state, the surface temperature was observed and recorded to be the same, allowing the sample emissivity to be determined as 0.68. When the chip was lit to measure T_j for four different currents, this very emissivity value was used.

APPENDIX E

For $\xi < 1$ (i. e. in the normal operation), we obtain R_{th} based on the thermal-resistance principle, namely $R_{th} = \Delta T / P_{th}$ (R_{th} denotes the thermal resistance, ΔT the junction gradient,

P_{th} the thermal power), which is used to extrapolate T_j for $\xi = 1$ (Figs. 3a and d).

Based on the first law of thermodynamics, we can obtain energy-conservation equations below:

$$\begin{cases} \dot{m}C_p\left(T_{j2} - T_{j1}\right) = P_{ele,12} & (S1) \\ \dot{m}C_p\left(T_{j3} - T_{j2}\right) = P_{ele,23} - P_{ph} & (S2) \\ \dot{m}C_p\left(T_{j4} - T_{j3}\right) = -\dot{Q}_{out} & (S3) \\ \dot{m}C_p\left(T_{j1} - T_{j4}\right) = \dot{Q}_{in}, & (S4) \end{cases}$$

where $T_{ji}(i = 1, 2, 3, 4)$ stands for the junction temperature at state i; $\dot{m}$ the mass; C_p the heat capacity.

According to the Ohmic heating (Fig. 2a), the minimum wasted thermal energy originates from a portion of electrical energy that consumed by electrons to overcome the barrier ($= IV_{net}$). Therefore, the minimum dissipated thermal power equals IV_{net}. Namely, $\dot{Q}_{out} = IV_{net}$. For illustration, in theory let us consider the case of $\xi = 1$ and $\dot{Q}_{in} = IV_{net} = 0.28$W, which a blue LED should absorb from the surroundings (have not realized in real life). In this condition, the portion of electricity $P_{ele,12}$ should push electrons to overcome the barrier, as a result $P_{ele,12} = IV_{net}$. Based on Eqs. (S1) and (S3), we obtained $T_{j2} + T_{j4} = T_{j1} + T_{j3}$. Since $\xi = 1$ implies $P_{ele} = P_{ph}$, we obtain $T_{j1} = T_{j3}$ according to Eqs. (S1) and (S2). Due to the fact that LED consists of a few different materials as shown in Fig.3d, it is difficult to discover the parameter of $\dot{m}$ and C_p. Hence, we obtained $T_{j2} = 315.70$K based on the thermal-resistance principle, namely $R_{th} = \Delta T / P_{th} = (T_{j2} - T_{sink})/\dot{Q}_{in}$. Therefore, we theoretically obtain $T_{j2} = 315.70$K, $T_{j4} = 280.60$K for $\xi = 1$ of a blue LED driven by $I = 350$ mA.

REFERENCES

[1] E. F. Schubert, *Light-Emitting Diodes*, 2nd ed. Cambridge, U.K.: Cambridge Univ. Press, 2006, ch. 5, pp. 98–100.

[2] W. Wang *et al.*, "High-efficiency vertical-structure GaN-based light-emitting diodes on Si substrates," *J. Mater. Chem. C*, vol. 25, no. 6, pp. 1642–1650, Feb. 2018. doi: 10.1039/C7TC04478J.

[3] H. T. Chen, Y. F. Cheung, H. W. Choi, S. C. Tan, and S. Y. Hui, "Reduction of thermal resistance and optical power loss using thin-film light-emitting diode (LED) structure," *IEEE Trans. Ind. Electron.*, vol. 62, no. 11, pp. 6925–6933, Nov. 2015. doi: 10.1109/TIE. 2015.2443106.

[4] J.-H. Zhang *et al.*, "Thermal analyses of alternating current light-emitting diodes," *Appl. Phys. Lett.*, vol. 103, p. 153505, Sep. 2013. doi: 10.1063/1.4823806.

[5] M. Soltani, M. Freyburger, R. Kulkarni, R. Mohr, T. Groezinger, and A. Zimmermann, "Reliability study and thermal performance of LEDs on molded interconnect devices (MID) and PCB," *IEEE Access*, vol. 6, pp. 51669–51679, Sep. 2018. doi: 10.1109/ACCESS.2018.2869017.

[6] K. J. Lee, S.-J. Kim, J.-J. Kim, K. Hwang, S.-T. Kim, and S.-J. Park, "Enhanced performance of InGaN/GaN multiple-quantum-well light-emitting diodes grown on nanoporous GaN layers," *Opt. Express*, vol. 22, no. S4, pp. A1164–A1173, Jun. 2014. doi: 10.1364/OE.22.0A1164.

[7] M.-H. Kim, "Origin of efficiency droop in GaN-based light-emitting diodes," *Appl. Phys. Lett.*, vol. 91, no. 18, Sep. 2007, Art. no. 183507. doi: 10.1063/1.2800290.

[8] Y.-L. Lee and W.-C. Liu, "Enhanced light extraction of GaN-based light-emitting diodes with a hybrid structure incorporating microhole arrays and textured sidewalls," *IEEE Trans. Electron Devices*, vol. 65, no. 8, pp. 3305–3310, Aug. 2018. doi: 10.1109/TED.2018.2849353.

[9] J. Tauc, "The share of thermal energy taken from the surroundings in the electro-luminescent energy radiated from ap-n junction," *Czech. J. Phys.*, vol. 7, pp. 275–276, Oct. 1957. doi: 10.1007/BF01688028.

[10] M. A. Weinstein, "Thermodynamic limitation on the conversion of heat into light," *J. Opt. Soc. Amer.*, vol. 50, no. 6, pp. 597–602, Jun. 1960, doi: 10.1364/JOSA.50.000597.

[11] P. Santhanam, D. J. Gray, Jr., and R. J. Ram, "Thermoelectrically pumped light-emitting diodes operating above unity efficiency," *Phys. Rev. Lett.*, vol. 108, Feb. 2012, Art. no. 097403, doi: 10.1103/hysRevLett.108.097403.

[12] P. Santhanam, D. Huang, R. J. Ram, M. A. Remennyi, and B. A. Matveev, "Room temperature thermo-electric pumping in mid-infrared light-emitting diodes," *Appl. Phys. Lett.*, vol. 103, Nov. 2013, Art. no. 183513. doi: 10.1063/1.4828566.

[13] M. Sheik-Bahae and R. I. Epstein, "Optical refrigeration," *Nature Photon.*, vol. 1, pp. 693–699, Dec. 2007. doi: 10.1038/nphoton.2007.

[14] P. W. Anderson, E. Abrahams, and T. V. Ramakrishnan, "Possible explanation of nonlinear conductivity in thin-film metal wires," *Phys. Rev. Lett.*, vol. 43, p. 718, Sep. 1979. doi: .10.1103/PhysRevLett.43.718.

[15] F. J. DiSalvo, "Thermoelectric cooling and power generation," *Science*, vol. 285, no. 5428, pp. 703–706, 1999. doi: 10.1126/science285.5428.703.

[16] M. J. Moran, H. N. Shapiro, D. D. Boettner, and M. B. Baileym, *Fundamentals of Engineering Thermodynamics*, 5th ed. Hoboken, NJ, USA: Wiley, 2006.

[17] S. Carnot, *Réflexions sur la puissance motrice du feu et sur les machines propres á développer cette puissance*, Paris, France: Bachelier, (in French), 1824.

[18] G. Pavlidis, D. Kendig, E. R. Heller, and S. Graham, "Transient thermal characterization of AlGaN/GaN HEMTs under pulsed biasing," *IEEE Trans. Electron Devices*, vol. 65, no. 5, pp. 1753–1758, May 2018, doi: 10.1109/TED.2018.2818621.

[19] J. P. Heremans, "The ugly duckling," *Nature*, vol. 508, pp. 327–328, Apr. 2014. doi: 10.1038/508327a.

[20] I. A. Martínez, É. Roldán, L. Dinis, D. Petrov, J. M. R. Parrondo, and R. A. Rica, "Brownian carnot engine," *Nature Phys.*, vol. 12, pp. 67–70, Oct. 2016. doi: 10.1038/nphys3518.

[21] T. M. Shih, *Numerical Heat Transfer*. New York, NY, USA: Springer-Verlag, 1984.

[22] J. Zhang, T. Shih, Y. Lu, H. Merlitz, R. R.-G. Chang, and Z. Chen, "Non-synchronization of lattice and carrier temperatures in light-emitting diodes," *Sci. Rep.*, vol. 6, Jan. 2016, Art. no. 19539, doi: 10.1038/srep19539.

[23] V. Székely, "A new evaluation method of thermal transient measurement results," *Microelectron. J.*, vol. 28, no. 3, pp. 277–292, 1997, doi: 10.1016/S0026-2692(96).

[24] M. Ha and S. Graham, "Development of a thermal resistance model for chip-on-board packaging of high power LED arrays," *Microelectron. Rel.*, vol. 52, pp. 836–844, May 2012. doi: 10.1016/j.microrel.2012.02.005.

JIHONG ZHANG received the B.S. degree in electron science and technology from the China University of Mining and Technology, Xuzhou, China, in 2010, and the Ph.D. degree from the Department of Electronic Science, Xiamen University, China, in 2015. Since 2015, she has been with the School of Electromechanical and Automotive Engineering, Yantai University, where she is currently an Assistant Professor. Her current research interests include solid-state lighting, solar cells, and micronanoscale heat transfer.

TIENMO SHIH received the B.S. degree in mechanical engineering from Taiwan University, in 1970, and the Ph.D. degree from the Department of Mechanical Engineering, University of California at Berkeley, in 1977. He became a Postdoctoral Fellow at Harvard University, in 1978. From 1978 to 2012, he taught and conducted research as an Associate Professor with The University of Maryland, College Park. From 2012 to 2018, he was a Professor with the Physics Department, Xiamen University. His current research interests include nanoscales and thermodynamics.

• • •